Published in final edited form as:
Mol Microbiol. 2009 August ; 73(4): 586–600. doi:10.1111/j.1365-2958.2009.06794.x.

Sinorhizobium meliloti CpdR1 is critical for coordinating cell-cycle progression and the symbiotic chronic infection

Hajime Kobayashi[†], **Nicole J. De Nisco**, **Peter Chien**, **Lyle A. Simmons**[§], and **Graham C. Walker**[*]
Department of Biology, Massachusetts Institute of Technology, 77, Massachusetts Avenue, Cambridge, MA 02139, USA

Abstract

ATP-driven proteolysis plays a major role in regulating the bacterial cell cycle, development and stress responses. In the nitrogen-fixing symbiosis with host plants, *Sinorhizobium meliloti* undergoes a profound cellular differentiation including endoreduplication of the genome. The regulatory mechanisms governing the alterations of the *S. meliloti* cell cycle *in planta* are largely unknown. Here, we report the characterization of two *cpdR* homologs, *cpdR*1 and *cpdR*2, of *S. meliloti* that encode single-domain response regulators. In *Caulobacter crescentus*, CpdR controls the polar localization of the ClpXP protease, thereby mediating the regulated proteolysis of key protein(s), such as CtrA, involved in cell-cycle progression. The *S. meliloti cpdR*1-null mutant can invade the host cytoplasm, however, the intracellular bacteria are unable to differentiate into bacteroids. We show that *S. meliloti* CpdR1 has a polar localization pattern and a role in ClpX positioning similar to *C. crescentus* CpdR, suggesting a conserved function of CpdR proteins among *f¿*-proteobacteria. However, in *S. meliloti*, free-living cells of the *cpdR*1-null mutant show a striking morphology of irregular coccoids and aberrant DNA replication. Thus, we demonstrate that CpdR1 mediates the coordination of cell-cycle events, which are critical for both the free-living cell division and the differentiation required for the chronic intracellular infection.

Introduction

Rhizobia are α-proteobacteria with the remarkable ability to form a nitrogen-fixing symbiosis with compatible legume hosts (reviewed in Broughton *et al*., 2000; Gibson *et al*., 2008; Jones *et al*., 2007). The symbiosis is based on chronic infection coordinated by the exchange of signal molecules between the symbiotic partners (reviewed in Jones *et al*., 2007; Kobayashi and Broughton, 2008; Perret *et al*., 2000). The process of infection of a plant host by rhizobia is comprised of multiple developmental stages, in which the bacteria modulate their cell proliferation in concert with the development of host cells (reviewed in Foucher and Kondorosi, 2000; Oke and Long, 1999). In the free-living stage, rhizobia cells divide in an asymmetric manner, producing two daughters of different sizes (Hallez *et al*., 2004; Lam *et al*., 2003). Upon recognition of a compatible host plant, rhizobia enter the root through host-derived tubes called infection threads (reviewed in Gage and Margolin, 2000; Gage, 2004). The extension of infection threads is synchronized with the colonization of rhizobia by the restriction of bacterial cell division and the collective movement of bacteria

[*]Corresponding author. Mailing address: Department of Biology, Massachusetts Institute of Technology, Cambridge, MA 02139. Phone: (617) 253-6711. Fax: (617) 253-2643. gwalker@mit.edu.
[†]Current address: Frontier Research Center for Energy and Resources, School of Engineering, The University of Tokyo, Eng. Bldg. #. 4, 7-3-1 Hongo, Bunkyo-ku, Tokyo 113-8656, Japan
[§]Current address: Department of Molecular, Cellular and Developmental Biology, University of Michigan. 830 N. University Ave. Ann Arbor MI 48109.

(Fournier *et al*., 2008; Gage, 2002). At the tip of the infection thread, the bacteria are released into the nodule cell by a process analogous to phagocytosis (reviewed in Brewin, 1998; Jones *et al*., 2007): the bacteria are engulfed with host-derived membranes (called peri-bacteroid membranes) and sealed off into membrane-bound vesicles (called symbiosomes) within the host cytoplasm, where the oxygen tension is reduced by leghemoglobin. The microoxic condition induces expression of genes encoding the nitrogenase and genes essential for microoxic respiration in rhizobia (reviewed in Kaminski *et al*., 1998). At the same time, the bacteria that have been newly released from the infection thread generally divide several times and then cease to divide upon initiation of nitrogen fixation (reviewed in Oke and Long, 1999). At this stage, the bacteria chronically infecting the host cytoplasm are referred to as bacteroids and act like plant organelles, where metabolites from both partners are interchanged (reviewed in Prell and Poole, 2006).

Sinorhizobium meliloti induces nodules of an indeterminate type on plants of *Medicago, Melilotus* and *Trigonella* genera (reviewed in Jones *et al*., 2007). In such indeterminate nodules, the bacterial symbionts undergo an even more striking cellular differentiation (Mergaert *et al*., 2006). In the process of the bacteroid development, DNA replication is repeated several times without cell division, resulting in the formation of elongated cells containing up to 24 copies of the genome. Fully differentiated bacteroids possess permeabilized cell envelopes and lose the ability to resume growth (Kobayashi *et al*., 2001; Mergaert *et al*., 2006). Although genes required for the symbiotic chronic infection have been actively studied in *S. meliloti* (reviewed in Gibson *et al*., 2008; Jones *et al*., 2007), the mechanism(s) governing the differentiation processes is largely unknown.

In several bacterial species, regulated proteolysis by ClpXP has been shown to control vital cellular processes (reviewed in Dougan *et al*., 2002; Jenal and Hengge-Aronis, 2003) including cell division (Jenal and Fuchs, 1998), cell differentiation (Liu *et al*., 1999) and nitrogen fixation (Rodriguez *et al*., 2006). ClpXP is an AAA+ protease, which is composed of the ClpX ATPase and the ClpP peptidase (reviewed in Baker and Sauer, 2006; Sauer *et al*., 2004). Substrates are initially recognized by ClpX and are subsequently unfolded and transferred to ClpP for degradation. In *Caulobacter crescentus*, a non-symbiotic member of α-proteobacteria, ClpXP proteolytically modulates the cellular level of CtrA (Chien *et al*., 2007; Gorbatyuk and Marczynski, 2005; Jenal and Fuchs, 1998; McGrath *et al*., 2006), an essential response regulator which regulates DNA replication and cell division (collectively, the progression of the cell cycle) (Laub *et al*., 2000; 2002; Quon *et al*., 1996; 1998). At least partially due to this role, ClpXP is essential for viability in *C. crescentus* (Jenal and Fuchs, 1998). *C. crescentus* shares several regulatory components (such as CtrA) involved in cell-cycle progression and differentiation with *S. meliloti* and its pathogenic relative *Brucella* species (Barnett *et al*., 2001; Bellefontaine *et al*., 2002; Hallez *et al*., 2004). It is therefore plausible that the ClpXP-mediated proteolysis might play a critical role in *S. meliloti* and its chronic infection.

Interestingly, during *C. crescentus* cell cycle, ClpXP dynamically localizes to the cell pole and the cell-division plane, providing temporal and spatial specificity to the proteolysis of substrates (McGrath *et al*., 2006). The proper localization of ClpXP is directed by another response regulator CpdR, which physically interacts with ClpXP, and is dependent on the phosphorylation state of CpdR (Iniesta *et al*., 2006). When CpdR is unphosphorylated, it localizes to the cell pole, thereby mediating ClpXP localization to the cell pole. When CpdR is phosphorylated, it and ClpXP are not localized to the cell pole and consequently CtrA is not degraded. The phosphorylation (thus, inactivation) of CpdR is mediated by the CckA-ChpT phosphorelay, in which the histidine kinase CckA phosphorylates the histidine phosphotransferase ChpT, which in turn phosphorylates CpdR (Biondi *et al*., 2006). The same phosphorelay also phosphorylates CtrA, which is in this case activated by the

phosphorylation. Thus, CpdR mediates the fine-tuning of the cell-cycle progression in *C. crescentus* by modulating the ClpXP-mediated proteolysis of CtrA (Biondi *et al*., 2006; Iniesta *et al*., 2006; 2008).

In this report, we investigated the role of CpdR in *S. meliloti* and present the first indication that proteolytic regulation and cell-cycle progression is critical for the chronic intracellular infection. The *S. meliloti* chromosome encodes two *cpdR* homologs (SMc04044 and SMc00720), designated *cpdR*1 and *cpdR*2. SMc04044 and SMc00720 do not appear to be in operons containing other ORFs (a tRNA-Val gene is located 285 bp downstream of SMc04044 and the insertion sequence ISRm22 is located downstream of SMc00720 in the opposite direction). Putative single domain-response regulators encoded by *cpdR*1 and *cpdR*2 share 61% and 46% amino-acid sequence identity with the CpdR protein of *C. crescentus* in the two pairwise comparisons, respectively, and share 42% amino-acid sequence identity with each other. We found that both *cpdR* homologs could be disrupted, while the *clpX* homolog was essential in *S. meliloti*. Only the *cpdR*1 mutant was symbiotically defective. Our examination of these mutants revealed that CpdR1 function is required for proper morphogenesis in free-living cells and for differentiation into bacteroids. We also found that CpdR1 functions to couple DNA replication to cell division in *S. meliloti*. In contrast to the *C. crescentus cpdR* mutant, which is poised at the G_1 phase of the cell cycle, the *S. meliloti cpdR*1 mutant accumulates more than two copies of genomic DNA, demonstrating the plasticity of this regulatory network among α-proteobacteria. Thus, in *S. meliloti*, cell division in the free-living stage and the bacteroid differentiation are controlled, in part, by CpdR1.

Results

Expression profiles of *cpdR* and *clpX* homologs in free-living and *in planta* cells of *S. meliloti*

To examine the role of the CpdR homologs in *S. meliloti*, we first determined their transcriptional expression during free-living growth and symbiosis. We also compared the expression profiles of the *cpdR* homologs and *clpX* by measuring their transcriptional expression in parallel. Chromosomal loci of *cpdR* genes (*cpdR*1 and *cpdR*2) and *clpX* were transcriptionally fused with *uidA* by inserting pJH104, an integration vector carrying promoter-less *uidA* (for *cpdR*1 and *cpdR*2) (Ferguson *et al*., 2005) or a *uidA*-Nm^r cassette (for *clpX*) (Metcalf and Wanner, 1993), downstream of each ORF (ATG of *uidA* were located 23, 23 and 59 bp downstream of the stop codons of *cpdR*1, *cpdR*2 and *clpX*, respectively), yielding strains Rm1021*cpdR*1*uidA*, Rm1021*cpdR*2*uidA* and Rm1021*clpXuidA*.

To measure expression in the free-living state, exponentially growing cells were inoculated into fresh M9 minimal media and β-glucuronidase activities of *S. meliloti* strains were monitored 1, 16, 24, 40, 48, 72 and 90 hours post subculture (Fig. 1, panel A). Both *cpdR*1 and *cpdR*2 fusions were expressed weakly throughout the growth phases. On the other hand, the expression of the *clpX* fusion was enhanced when cells entered stationary phase.

In order to study gene expression during symbiosis, nodules elicited on alfalfa by the strains carrying *uidA* fusions were sectioned and stained for β-glucuronidase activity (Fig. 1, panel B–C). *S. meliloti* induces formation of indeterminate-type nodules with persistent meristems (which are marked with asterisks in Fig. 1, panel B–C). Expression of *clpX* and the *cpdR* fusions occurs throughout the nodule. This is consistent with the possibility that the CpdR proteins as well as ClpX are present throughout symbiotic development and could potentially play a role in multiple stages of symbiosis.

CpdR1 localizes to cell poles

Since our assay with *uidA*-transcriptional fusions indicated that two *cpdR* homologs are transcribed (albeit at a low level) in *S. meliloti*, we asked if both of the CpdR proteins share the same function with *C. crescentus* CpdR; localization to the cell pole and recruitment of ClpXP. To this end, the localization of CpdR1 and CpdR2 was examined. We fused *yfpmut2A206K* (encoding a monomeric derivative of YFP, and referred to herein as *yfp*) to *cpdR*1 and *cpdR*2 under the control of their native promoters on the low-copy vector pTH1227 (Cheng *et al*., 2007). Resulting plasmids, p-*cpdR*1-*yfp* and p-*cpdR*2-*yfp*, carrying *cpdR-yfp* fusion genes were introduced into the wild-type *S. meliloti* strain Rm1021.

In the log-phase cells, a single CpdR1-YFP focus was visible above the background fluorescence in ~6% of cells (n=1399) (Fig. 2A–C; Table 1). In *C. crescentus*, it has been reported that the CpdR focus only appears at particular stages of the cell cycle (the swarmer-to-stalked cell transition and the predivisional stage) (Iniesta *et al*., 2006). Since the *S. meliloti* cultures were not synchronized, it is reasonable to speculate that the cultures consisted of a heterogeneous cell population, where ~6% of cells were at the cell-cycle stage(s) specific for polar localization of CpdR1. The formation of CpdR1-YFP foci was also observed in ~5% (n = 1273) of cells in stationary phase, although the YFP foci signal was faint compared to the foci intensity of cells in log phase (Fig. 2D–F; Table 1). Of the foci that formed, ~100% (n = 245) of the CpdR1-YFP foci were localized at the cell poles (Supplemental Table S1) and we did not detect any cells with more than one focus (this is similar to *C. crescentus*) (Table 1).

We also investigated the localization of CpdR2-YFP in *S. meliloti.* We found that the formation of CpdR2-YFP foci was observed in only a small subpopulation of stationary-phase cells (~0.4% of cells, n = 561; Table 2). In both log- and stationary-phase cultures, some of cells have brighter CpdR2-YFP signals throughout the cell than other cells (Fig. 2G–L). It should be noted that each YFP fusion was transcribed from the native promoters of *cpdR*1 and *cpdR*2 respectively, supporting our results with *uidA* fusions showing that *cpdR*1 and *cpdR*2 were expressed throughout the growth phases. The active localization of CpdR1 to cell poles suggested that CpdR1 shares a similar function with *C. crescentus* CpdR, while the significance of CpdR2 localization remains unclear.

*S. meliloti cpdR*1 and *cpdR2* are not essential, while *clpX* provides an essential function

To further examine the function of *cpdR*1 and *cpdR*2 in *S. meliloti*, both were disrupted by inserting a spectinomycin/streptomycin resistance gene (for *cpdR*1) (Fellay *et al*., 1987) or a *uidA*-Cm^r cassette (for *cpdR*2) (Metcalf and Wanner, 1993), generating strains Rm1021Ω*cpdR*1 and Rm1021*cpdR*2::*uidA*. The *cpdR*1-null mutant grew much slower than the parental strain, while the growth of the *cpdR*2-null mutant was virtually indistinguishable from that of the parental strain (data not shown). This further supports the idea that the two *cpdR* homologs have non-identical roles in *S. meliloti*. In addition, we found that *clpX* is essential for viability of *S. meliloti*, as is the case for *C. crescentus* (Jenal and Fuchs, 1998). We attempted to generate a *clpX*-null allele in *S. meliloti*. The plasmid, pJQ-*clpX*$^-$, a suicide vector pJQ200-SK (Quandt and Hynes, 1993) derivative in which the *clpX* ORF was disrupted by insertion of a neomycin resistance (Nm^r) marker (Fellay *et al*., 1987), was integrated into the chromosomal *clpX* locus by single-crossover. Counter-selection for the double-crossover in the resulting strain was performed with derivatives that contained either a plasmid carrying the functional copy of *clpX* (p-*clpX*$^+$) or the empty vector pTH1227. The disruption of chromosomal *clpX* occurred only in the presence of p-*clpX*$^+$ (data not shown), indicating that *clpX* encodes an essential function in *S. meliloti*. Similar procedures were employed to show that *ctrA* and *ccrM*, genes encoding proteins critical for cell-cycle progression, are also essential in *S. meliloti* (Barnett *et al*., 2001;

Wright *et al*., 1997). We conclude that CpdR1 has an important role during the free-living growth of *S. meliloti* and that *clpX* is essential under the growth conditions examined in this study. We speculate that the role of CpdR in free-living *S. meliloti* likely involves the regulation of ClpXP protease as reported for *C. crescentus* CpdR (Iniesta *et al*., 2006).

CpdR1 is critical for the bacteroid differentiation

To test whether the *cpdR* homologs are important for symbiosis, alfalfa seedlings were inoculated with the *cpdR*1- or *cpdR*2-null mutants. Four weeks post inoculation, alfalfa plants infected with the wild type grew to a shoot length of 11.4 ± 0.3 cm with pink-colored and elongated nodules on the roots (Fig. 3A). In contrast, plants inoculated with the *cpdR*1-null mutant appeared to be starved of nitrogen, having short shoots (2.9 ± 0.1 cm) with yellowed leaves (Fig. 3A). Nodules induced by the *cpdR*1-null mutant were white-colored, small and non-elongated globular shape. The size and appearance of the shoots of the plants were indistinguishable from those of the mock-inoculated plants, which had no nodules on their roots. This could indicate that the nodules induced by the *cpdR*1-null mutant lacked nitrogen-fixing activity (Fig. 3A). No significant difference was observed in nodule number or in plant growth between plants infected with the wild type and the *cpdR*2-null mutant (Fig. 3A).

A more striking phenotype of the *cpdR*1-null mutant was observed by electron microscopy. Fig. 3B and D shows a plant cell from the nitrogen-fixing zone of a nodule containing the wild-type *S. meliloti* strain Rm1021. These bacteroids generally have elongated or Y-shaped morphology and are five to ten times longer than the free-living cells. Fig. 3C and E show the corresponding region of a nodule containing the *cpdR*1-null mutant. The host cells contain numerous intracellular bacteria, indicating that the *cpdR*1-null mutant is not especially impaired in the early stages of nodule invasion through the root hair or in invading the cytoplasm of the host cell. However, the morphology of these intracellular bacteria is diverse. Although some cells are abnormally enlarged, most of the bacteria appear to be highly irregular spherically-shaped (coccoid) cells much smaller than the bacteroids of the wild-type *S. meliloti* Rm1021 and have refractory cytoplasm indicative of aborting bacteroids (Campbell *et al*., 2002). The host cells also contained large amyloplasts. Amyloplasts are starch deposits that are normally present in nodule cells early in development and are absorbed upon *S. meliloti* infection of alfalfa. Thus, in *S. meliloti*, CpdR1 is critical for establishing the chronic intracellular infection, particularly, at the stage of bacteroid differentiation.

The symbiotic deficiency of the *cpdR*1-null mutant was fully complemented by p-*cpdR*1^{+}, a plasmid carrying the wild-type *cpdR*1^{+}, and also by p-*cpdR*1-*yfp*, but not by the empty vector pTH1227. In *C. crescentus*, it has been shown that the activity of CpdR is regulated by phosphorylation (Iniesta *et al*., 2006). Only the unphosphorylated CpdR localizes to the cell pole and is capable of directing the polar localization of ClpXP. To understandthe role of CpdR phosphorylation status in symbiosis, we generated an allele of *cpdR*1, *cpdR1D53A*, that codes for an alanine at position 53 instead of the conserved aspartic acid. In *C. crescentus*, CpdRD51A, the analog of *S. meliloti* CpdR1D53A, was shown to prevent phosphorylation of the protein, resulting in a constitutively active form that directs ClpXP to the cell pole throughout the cell cycle (Iniesta *et al*., 2006). Introduction of the *cpdR1D53A* allele did not restore the symbiotic deficiency of the *cpdR*1-null mutant (Fig. 3A), indicating that the fine-tuning of CpdR1 phosphorylation status is important for symbiosis. Heterologous expression of *C. crescentus cpdR* in the *S. meliloti cpdR*1-null background complements the symbiotic deficiency as well as the growth defect of the free-living cells, indicating that the CpdR function is conserved between *S. meliloti* and *C. crescentus*. We conclude that *S. meliloti* CpdR1 phosphorylation is critical for its function and that *C.*

crescentus cpdR can complement the *S. meliloti cpdR*1 defect indicating a conserved role of CpdR among α-proteobacteria.

CpdR1 is required for proper morphogenesis of *S. meliloti*

The abnormal morphology of the intracellular cells of the *cpdR*1-null mutant in alfalfa led us to examine the cell morphology in the free-living stage. As free-living cells, the wild-type *S. meliloti* are rod shaped (Fig. 4A). Strikingly, free-living cells of the *cpdR*1-null mutant are highly irregular swollen or coccoid shape with the size generally three to four times larger than the size of wild-type *S. meliloti* cells (Fig. 4B). Some of cells were further enlarged and branched with single or multiple asymmetric septa (data not shown). The morphology, and the size of the free-living cells of the *cpdR*1-null mutant, was similar to those of the *in planta* intracellular cells. This suggests that the *cpdR*1-null mutant could not initiate the differentiation process into bacteroid form. Introduction of the wild-type *cpdR*1^{+} to the *cpdR*1-null mutant restored normal morphology (Fig. 4C), while introduction of the *C. crescentus cpdR* only partially rescued the morphological defect (Fig. 4D). The *S. meliloti cpdR*1-null mutant expressing *C. crescentus* CpdR appeared to be rod shaped with, occasionally, single or multiple small branches (Fig. 4D). Introduction of the *cpdR1D53A* allele into the *cpdR*1-null mutant failed to rescue the morphology of the mutant and exacerbated slow growth phenotype (Fig. 4F; data not shown). Moreover, expression of *cpdR1D53A* in the wild-type *S. meliloti* Rm1021 transformed ~6% (n = 551) of the cells into highly branched cells with more than three poles (Fig. 4G; Table 2). Such cells were not detected in the wild-type *S. meliloti* carrying the empty vector (n = 413) or in the wild-type *S. meliloti* alone (Table 2). Thus, CpdR1 function is critical for the proper morphogenesis during both free-living growth and during bacteroid differentiation. The morphology of the *cpdR*2-null mutant was indistinguishable from the wild-type *S. meliloti* Rm1021 (Fig. 4E), indicating that *cpdR*2 is not important for cell morphogenesis in the free-living form.

The morphological phenotype caused by CpdR1D53A is Min dependent

During the examination of morphology of free-living cells, we noticed that the morphology of the *cpdR*1-null mutant is similar to the morphology of the *minE*-disrupted mutant of *S. meliloti* (Cheng *et al*., 2007). The MinE protein forms, together with MinC and MinD, the Min cell-division inhibitor system. The Min system is well studied in *E. coli*, where it directs cell division to the mid-cell by negatively regulating the formation of the Z ring (reviewed in Margolin, 2005). MinC is the inhibitor of Z-ring formation, which is recruited to the membrane by MinD and induced to oscillate by MinE. Although the *minE* single mutant shows a morphological defect, the *minCDE* triple mutant has wild-type morphology in *S. meliloti*, indicating that the phenotype of the *minE* mutant is likely due to the nonspecific action of MinC and MinD (Cheng *et al*., 2007; Fig. 4H; Table 2). Overexpression of MinD or MinCDE in *S. meliloti* generates highly branched cells (Cheng *et al*., 2007), which is also similar to the morphology we observe with *S. meliloti* Rm1021 expressing CpdR1D53A (Fig. 4G).

The similarity in morphology between the *cpdR*1-null mutant and the *minE*-null mutant, as well as between the CpdR1D53A-expressing strain and Min-overexpressing strains, led us to hypothesize that *cpdR* affects proper activity of the Min system. To test this hypothesis, *minCDE* were disrupted in the *cpdR*-null and *cpdRD53A* backgrounds. Disruption of *minCDE* did not restore the morphology of the *cpdR*1-null mutant (Fig. 4I), indicating that the morphological defect of the *cpdR*1-null mutant is independent of the Min system. However, when *minCDE* was disrupted in *S. meliloti* Rm1021(p-*cpdR*1*D53A*), highly branched cell (with more than three poles) was not detected any longer, while elongated cells (with two or three poles) were still observed (Fig. 4J; Table 2). Thus, the

morphogenesis of highly branched cells by CpdR1D53A appears to depend, in part, on the Min system.

CpdR1 affects the formation of ClpX-YFP foci

C. crescentus cpdR can partially complement the *S. meliloti cpdR*1-null mutant, suggesting that the molecular function is conserved for both gene products. In *C. crescentus*, the role of CpdR in directing ClpX to the cell pole has been demonstrated (Iniesta et al., 2006). To examine the role of CpdR1 in the ClpX localization, we fused *yfp* to the genomic copy of *clpX* in *S. meliloti*. The strain, Rm1021*clpX-yfp*, which carries the *clpX-yfp* fusion gene as the only copy of *clpX*, is viable. The growth rate and the cell morphology of the *clpX-yfp* strain was indistinguishable from the wild-type *S. meliloti* strain Rm1021, indicating that the ClpX-YFP fusion protein is functional. In logarithmic-phase growth, ~9% (n = 1005) of cells had one focus of ClpX-YFP visible above the background fluorescence (Fig. 5A–C; Table 3). In stationary-phase cells, ClpX-YFP foci formed in ~88% (n = 594) of cells (Fig. 5D–F; Table 3). Most of the cells containing ClpX-YFP foci had one focus per cell (Table 3). This observation is interesting, since CpdR1-YFP foci were observed in ~5% (n = 1273) of cells in stationary phase (Table 1). Thus, in stationary-phase cells, most of the population of cells with ClpX-YFP foci do not correspond to the population of cells with CpdR1-YFP foci. In both growth phases, ClpX-YFP foci were preferentially formed at the cell poles. We found that ~78% (n = 134) and ~97% (n = 150) of ClpX-YFP foci were located at the poles in logarithmic- and stationary-phase cells, respectively (Table S2). Interestingly, ClpX-YFP foci were observed in less than ~1% of mature bacteroids (n = 579). Taken together, these observations indicate that ClpX-YFP foci formation is growth-phase regulated.

To assess the role of two CpdR homologs in directing ClpX to the cell pole, the localization of ClpX-YFP was examined in the *cpdR*1- and *cpdR*2-null mutants. Compared to the wild-type, a smaller population of the *cpdR*1-null cells showed ClpX-YFP foci (Fig. 5J–O; Table 3). We found that the percentage of stationary-phase cells with ClpX-YFP foci was reduced ~eight-fold in the *cpdR*1-null mutant (Table 3). In *C. crescentus*, it has been reported that ClpX localization to the cell-division plane is independent of CpdR function (Iniesta *et al*., 2006). It has to be noted that, since we cannot distinguish the cell-division plane of *S. meliloti* (it is difficult to determine by DIC microscopy whether two proximal cells are currently dividing or just placed side by side), we can only score the location of foci as “polar” when they are located at the fully formed pole of a cell (Supplementary Table S2). The decreased formation of ClpX foci in the *cpdR*1-null mutant further supports the hypothesis that CpdR1 plays a conserved role in the polar localization of ClpX in *S. meliloti*. We could not score the location of ClpX foci in the *cpdR*1-null mutant, because the “poles” were not obvious in the irregular coccoid cells. In the *cpdR*1-null mutant, we also noticed that the foci intensity of ClpX-YFP was reduced relative to that of the foci formed in the wild-type background. In the wild-type background, ClpX-YFP foci were readily captured by an exposure for 240 milliseconds, while an exposure of 6000 milliseconds was necessary to capture distinct foci in the *cpdR*1-null mutant. This observation suggests that the loss of CpdR1 function pleiotropically affects the ClpX expression and/or the accumulation of ClpX-YFP at the cell poles.

We also examined the effect of CpdR1D53A on ClpX localization in *S. meliloti*. In the wild-type *S. meliloti* Rm1021 expressing CpdR1D53A, cell morphologies are abnormal (see Fig. 4G), but the formation and the localization of ClpX-YFP foci nonetheless showed common features with background Rm1021: a minority of cells formed a ClpX focus, and of those that did, the foci were at cell poles (Fig. 5P–R; Table S2). These observations differ from results in *C. crescentus* (Iniesta *et al*., 2006), where the expression of CpdRD51A resulted in ~100% polar localization of ClpX foci. This difference is probably because we expressed plasmid-born *cpdR*1*D53A* under the control of a *tac* promoter in the wild-type *S. meliloti*

Rm1021, where the wild-type *cpdR* gene is also present. In the *C. crescentus* strain, however, *cpdRD51A* replaces the wild-type *cpdR* locus and was expressed from the native *cpdR* promoter (Iniesta *et al*., 2006). We did not examine localization of ClpX-YFP in the *cpdR*1-null mutant expressing CpdR1D53A, since the morphology of the cells was severely defective (data not shown). In the *cpdR*2-null mutant or the wild-type *S. meliloti* expressing CpdR2D53A, cells formed ClpX-YFP foci of intensity indistinguishable from the foci in wild-type cells, although the population of cells with ClpX-YFP foci was slightly affected compared to the wild-type *S. meliloti* background (Fig. S1; Table 3). We conclude that CpdR1 is important for proper subcellular localization of ClpX-YFP in *S. meliloti*.

CpdR1 functions to coordinate initiation of DNA replication with cell-cycle progression

In *S. meliloti*, it has been shown that the larger cell volume correlates with the polyploid state of the cell (Mergaert *et al*., 2006). The enlarged cell volume of the *cpdR*1-null mutant led us to examine the DNA content of *S. meliloti* cells. Flow cytometry is a well-established tool for studying the cell cycle in synchronized cultures of *C. crescentus* (Winzeler and Shapiro, 1995). It has also been used in *S. meliloti* to examine the state of chromosomal replication in cell populations (Mergaert *et al*., 2006; Wright *et al*., 1997). As reported previously (Mergaert *et al*., 2006), in the wild-type *S. meliloti* strain Rm1021, DNA content distribution of an exponentially growing cell population is composed of two peaks (Fig. 6A). The first (left) peak indicates the number of cells with 1C DNA content (marked with blue-dotted line). The second peak is positioned around twice the relative fluorescence intensity of the first peak and represents the cells with 2C DNA content (marked with red-dotted line). In the *cpdR*1-null mutant, one broad peak representing cells with more than one genome (mainly 2~5C) equivalents were observed (Fig. 6B), indicating that most cells had multiple copies of the genome. Thus, in the *cpdR*1-null mutant, aberrant DNA replication uncoupled from cell division seems to have occurred. Introduction of the wild-type *cpdR*1^{+} restored proper progression of cell cycle in the *cpdR*1-null mutant (Fig. 6C). The profile of DNA content distribution of the *cpdR*1-null mutant expressing *C. crescentus* CpdR was similar to the profile in the wild-type, although the population with 2C DNA content was larger than the population with 1C DNA content (Fig. 6D).

This observation, together with the partially-rescued morphology of the *S. meliloti cpdR*1-null mutant by *C. crescentus cpdR*, suggests that *C. crescentus* CpdR is partially functional in *S. meliloti*. *C. crescentus* CpdR likely has a different affinity for *S. meliloti* ChpT and ClpX, causing a slight perturbation in progression of the *S. meliloti* cell cycle. In the wild-type *S. meliloti* expressing CpdR1D53A, the population with 2C DNA content was also larger than the population with 1C DNA content (Fig. 6F). In this strain, moreover, populations with 2~5C DNA content were also detected, likely corresponding to the cells with elongated or highly branched morphology. The DNA content profile of the *cpdR*1-null mutant expressing CpdR1D53A was indistinguishable from the *cpdR*1-null mutant with the empty vector or the mutant alone (Fig. 6E and G). Thus, expression of CpdR1D53A also causes aberrant cell-cycle progression and the effect of CpdR1D53A expression requires the presence of wild-type *cpdR*1^{+}. The *cpdR*2-null mutant showed DNA content profile indistinguishable from the wild-type *S. meliloti* Rm1021 (Fig. 6H). These data suggest that the function of CpdR1 is critical for proper coupling of DNA replication with cell division in *S. meliloti*.

Discussion

In this study, we demonstrate that CpdR plays a critical role in *S. meliloti*. In the free-living stage, cells of the *cpdR*1-null mutant showed an irregular coccoid morphology instead of the rod shape of the parental strain. The cells are generally three to four times larger in volume than wild-type cells. In *S. meliloti*, it has been shown that the larger cell volume correlates

with the polyploid state of a cell (Mergaert *et al*., 2006). Strikingly, the *cpdR*1-null mutant tends to accumulate higher copies (generally 2~5C) of genomic DNA. Thus, in *S. meliloti*, the loss of CpdR1 function results in uncoupling between DNA replication and cell division, causing a higher genomic content and enlarged spherical morphology of the mutant cells.

Moreover, we demonstrate that CpdR1 is required for symbiosis between *S. meliloti* and the host plant alfalfa. Upon inoculation in alfalfa, the *cpdR*1-null mutant is capable of inducing the formation of nodules on the root and capable of invading the cytoplasm of nodule cells. However, it appears that nitrogen fixation does not occur in the resulting nodules. In these nodules, the intracellular bacteria remain morphologically similar to the free-living cells of the *cpdR*1-null mutant and do not differentiate into wild-type bacteroids, which are normally larger and elongated. In wild-type *S. meliloti*, elongation of the bacteria during bacteroid maturation is a result of repeated DNA replication without cell division (endoreduplication) (Mergaert *et al*., 2006). The inability of intracellular cells to differentiate into bacteroids indicates that, in the *cpdR*1-null mutant, normal endoreduplication required for bacteroid differentiation is not initiated. Thus, in the *cpdR*1-null mutant, the loss of proper cell-cycle control is likely a common cause of both the aberrant morphology in the free-living stage and a defect in bacteroid differentiation. In other words, the same regulatory mechanism involving CpdR1, which couples initiation of DNA replication to cell division in free-living stage, also affects the endoreduplication during bacteroid development.

What is the molecular function of CpdR1 critical for coordinating cell-cycle progression? In *C. crescentus*, CpdR directs ClpXP complex to the cell pole, thereby mediating regulated proteolysis of ClpXP substrates (Iniesta *et al*., 2006). The cross-species complementation of *S. meliloti* CpdR1 with *C. crescentus* CpdR strongly suggests a conserved role for CpdR homologs between α-proteobacterial species. In agreement with this idea, we observed that loss of CpdR1 function attenuates the polar localization of ClpX-YFP.

It is therefore likely that the phenotype of the *cpdR*1-null mutant is caused by a lack of proper proteolysis by ClpXP. In *C. crescentus*, CtrA is an important substrate of ClpXP (Chien *et al*., 2007; Gorbatyuk and Marczynski, 2005; Jenal and Fuchs, 1998). CtrA controls, directly or indirectly, critical cell-cycle regulated genes including those involved in polar morphogenesis, DNA replication initiation, DNA methylation, cell division, and cell wall metabolism (Laub *et al*., 2002). CtrA is conserved in *S. meliloti* and it has been shown that *C. crescentus ctrA* can substitute for *S. meliloti ctrA* for viability (Barnett *et al*., 2001). CtrA protein of *S. meliloti* has a conserved ClpX-recognition signal at the C terminus (Flynn *et al*., 2003; Chien *et al*., 2007), suggesting that CtrA is also a substrate for ClpXP in *S. meliloti*. Modified abundance of CtrA affects cell-cycle progression (Quon *et al*., 1998) and at least partially accounts for aberrant cell-cycle progression in the absence of *cpdR*1 in *S. meliloti*.

Regarding cell-cycle progression, the phenotype of the *cpdR*1-null mutant fundamentally differs in *S. meliloti* from the phenotype reported in the *C. crescentus cpdR*-null mutant. In *C. crescentus*, the *cpdR*-null mutant also showed an aberrant morphology; an abnormal location of the cell-division plane and straight-cell morphology rather than the crescentoid morphology of the wild-type (Iniesta *et al*., 2006). It has also been reported that disruption of *C. crescentus cpdR* results in decreased motility, a longer generation time and, in a subpopulation, elongation of the cell (Skerker and Laub, 2005). In *S. meliloti*, on the other hand, we found that a disruption of *cpdR*1 results in significant enlargement of the cell size and spherical cell shape in most of the cells. More importantly, the loss of CpdR function does not cause polyploidy in *C. crescentus* (Duerig *et al*., 2009).

The different phenotypes resulted from loss of CpdR function on DNA replication likely reflects the plasticity of the regulation network involving CtrA in α-proteobacterial species (Hallez *et al*., 2004). In *C. crescentus*, phosphorylated CtrA (CtrA~P) binds to five distinct sites in the origin of replication to repress replication initiation by blocking the access of proteins for DNA replication initiation (Quon *et al*., 1998; Siam and Marczynski, 2000). CpdR directs ClpXP to the pole, where ClpXP degrades the CtrA~P, allowing for de-repression of DNA replication initiation. In the absence of CpdR, the ClpXP protease is not positioned at the pole and, consequently, CtrA~P is not degraded, keeping the replication origin physically blocked and DNA replication initiation repressed. Yet, CpdR is not essential for viability most likely because CtrA~P could still be inactivated by dephosphorylation.

In *S. meliloti*, on the other hand, no conserved CtrA-binding site has been detected in the replication origin (Hallez *et al*., 2004). In *Brucella abortus*, an intracellular pathogen closely related to *S. meliloti*, the replication origin also lacks a functional CtrA-binding site and was shown not to be bound by *B. abortus* CtrA *in vitro* (Bellefontaine *et al*., 2002). From these observations, it has been proposed that, in *S. meliloti* and *B. abortus*, DNA replication initiation is not regulated by the binding of CtrA to the replication origin (Bellefontaine *et al*., 2002; Hallez *et al*., 2004). It is therefore likely that, in the absence of CpdR function, the replication origin is available for DNA replication initiation even though CtrA is not proteolytically regulated. In agreement with this model, we found that, in *S. meliloti*, the loss of CpdR1 function does not result in repression of DNA replication initiation and can even provoke DNA replication in an unregulated manner.

We find it likely that genes regulated by CtrA are misregulated by the stabilization of CtrA and at least partially responsible for the aberrant cell-cycle progression in the *cpdR*1-null mutant. In *S. meliloti* and *C. crescentus*, it has been reported that overexpression of *ccrM*, a CtrA-target gene encoding a DNA methyltransferase, results in the loss of control of DNA replication and aberrant cell morphology, phenotypes similar to the *cpdR*1-null mutant (Wright *et al*., 1996; 1997; Zweiger *et al*., 1994). Although the accumulation of CcrM protein was not observed in the *C. crescentus cpdR* mutant (Iniesta *et al*., 2006), it is possible that *ccrM* is overexpressed in the *S. meliloti cpdR*1 mutant, contributing to its phenotype. In the *S. meliloti* symbiotic plasmid pSymA, putative CtrA-binding sites have been detected in promoter regions of *repA*2 (Hallez *et al*., 2004), which encodes a putative replication protein A. Unregulated expression of *repA2* could also be the cause of the aberrant DNA replication in the *cpdR*1-null mutant.

In *S. meliloti* and *B. abortus*, two and four CtrA-binding motifs were detected in an upstream region of the *minCDE* operon, respectively, while *minCDE* is absent in *C. crescentus* genome (Bellefontaine *et al*., 2002; Hallez *et al*., 2004; Cheng *et al*., 2007). When CpdR1D53A, the constitutively active variant of CpdR1, is expressed in *S. meliloti*, *minCDE* is probably de-repressed, causing the over-branched cell morphology of the strain. The over-branched cell phenotype was only seen in cells expressing CpdR1D53A in the presence of wild-type *cpdR*1^{+}. It is unclear how the effect of CpdR1D53A expression requires the wild-type *cpdR*1^{+} in *S. meliloti*.

In addition to the perturbation in cell-cycle progression, abundance of other ClpXP substrates as a consequence of reduced ClpXP localization may contribute to the phenotype of the *cpdR*1-null mutant. It has been shown that ClpXP plays a major role in protein quality control by degrading SsrA-tagged proteins (Gottesman *et al*., 1998; Herman *et al*., 1998; Keiler *et al*., 1996). The SsrA tag is a peptide that is added co-translationally to the C termini of nascent polypeptides in stalled translation complexes, and targets these proteins for degradation by ClpXP and other proteases (Keiler *et al*., 1996). It is possible that SsrA-

tagged proteins are not properly degraded by ClpXP in the absence of CpdR1, contributing to the pleiotropic phenotype of the *cpdR*1-null mutant. In agreement with this idea, the *Bradyrhizobium japonicum sra* locus, which encodes a *ssrA* homolog, is essential for symbiosis with the host plant (Ebeling *et al*., 1991).

We observed that the majority (~88%) of cells contain ClpX-YFP foci in stationary phase cells, while ClpX-YFP foci were observed in around ~10% of cells in logarithmic phase. Such increased formation of ClpX foci in stationary phase has not been reported in other organisms. The localization of ClpX has been examined in *C. crescentus* and the Gram-positive bacteria *Bacillus subtilis* (Kain *et al*., 2008; Kirstein *et al*., 2008; McGrath *et al*., 2006; Simmons *et al*., 2008). In the case of *C. crescentus*, however, the localization was not examined in stationary phase. In *B. subtilis*, a *cpdR* homolog has not been identified, and ClpX-GFP forms foci preferentially at the poles in approximately half of cells (Simmons *et al*., 2008). The percentage of cells with ClpX foci remains constant from logarithmic phase to stationary phase (L.A. Simmons, unpublished). Thus, our observation suggests that, in *S. meliloti*, ClpXP-dependent proteolysis plays an important role during stationary phase, in addition to its role in the cell-cycle progression. In *E. coli*, it has been reported that cultures of the strains lacking functional ClpP or ClpX displayed a more rapid loss of viability during extended stationary phase than the wild type (Weichart *et al*., 2003). It is interesting to note that the *cpdR*1-null mutant displays decreased foci formation of ClpX also in stationary phase cells, suggesting that CpdR1 function is required for the ClpX localization in both growth phases.

Thus, further study is required to determine the molecular function of CpdR1 and ClpXP in *S. meliloti*. Moreover, the genome of *S. meliloti* encodes the second homolog of *cpdR*, *cpdR*2, and three *clpP* homologs. Although we could not detect a phenotype of the *cpdR*2-null mutant, CpdR, ClpX and ClpP proteins may form a network, which regulates various physiological processes in the complex life cycle of *S. meliloti*. As we discussed above, since the regulatory network involving CtrA in *S. meliloti* and *Brucella* species share a similar structure (Hallez *et al*., 2004), the CpdR protein may also have a critical role in coordinating cell-cycle progression in *Brucella* species. It would be interesting to examine whether CpdR is also critical for the chronic infection of *Brucella* species.

Experimental procedures

Microbiological techniques

Strains and plasmids used in this study are listed in Supplemental Table S3. *E. coli* recombinants were grown at 37°C on Luria-Bertani media/medium (Sambrook *et al.*, 1989). *S. meliloti* strain Rm1021 and its derivatives were raised at 30°C in/on M9 succinate medium with biotin or LBMC (LB supplemented with 2.5 mM MgSO4 and 2.5 mM CaCl2). Gentamycin (Gm), neomycin (Nm), streptomycin (Sp), streptomycin (Sm), and tetracycline (Tet) were added at concentrations of 50, 200, 50, 500 and 15 μg ml^{-1}, respectively. Plasmids were mobilized into *S. meliloti* strain Rm1021 and derivative strains by tri-parental mating using pRK600 as the helper plasmid (Ditta *et al.*, 1980). Pfu turbo (Stratagene) was used in all PCR reaction followed by cloning. The amplified products were cloned into pCR-Blunt II-TOPO (Invitrogen) and verified by sequencing the inserts.

Construction of insertional disruptions of *clpX* and *cpdR* homologs

To construct the insertional disruption of *cpdR*1 (SMc04044), *cpdR*2 (SMc00720) and *clpX*, we amplified each full-length ORF with flanking regions by PCR using Rm1021 genomic DNA and the following primer pairs: for *cpdR*1 (5′-CTCGAGAAACGTGGCGCTGCGGAACAGTTCATCGACGAAAT-3′/5′-

CTGCAGTTCCGTCGAGCGCGCTAAGGCGTTGAAATAACGAA-3′); for *cpdR*2 (5′-CCCGGGACCGAATCCAAGGGCGTCAGGATCACCAAGGATAT-3′/5′-TCTAGAGCGCTACGGCCTTGCGGATGTCGGGCAGTGAAAAT-3′); for *clpX* (5′-TTGCGGCAAGAGCCAGCATGAAGTCCGC-3′/5′-ATGCTGTTGCAGACCTTGCGACCTGCCC-3′). Underlined nucleotides correspond to mismatches introduced to create selected restriction sites. To disrupt *cpdR*1, *cpdR*2 and *clpX*, a Sm^r/Sp^r cassette (from pHP45Ω; Fellay *et al*., 1987), an *uidA*-Cm^r cassette (from pWM4; Metcalf and Wanner, 1993) and a Km^r/Nm^r cassette (from pHP45Ω-Km; Fellay *et al*., 1987) were inserted into the internal *Nru*I, *Sal*I and *Bgl*II sites, respectively. DNA fragments containing disrupted *cpdR* and *clpX* homologs were sub-cloned into pJQ200-SK (Quandt and Hynes, 1993), and the resulting plasmids were mobilized into Rm1021 or its derivatives by tri-parental mating. Transconjugants were first selected on LBMC plates containing Sm and Gm, then on LBMC plates containing appropriate antibiotics to select the antibiotic-resistance markers in the disrupted genes and 5% (w/v) sucrose to select for double crossovers. Replacement of wild-type *clpX* and *cpdR* genes with its disrupted loci was confirmed by PCR.

Construction of plasmids for expression of CpdR proteins, ClpX and CpdR variants

The *cpdR*1, *cpdR*2 and *clpX* genes were PCR amplified by using Rm1021 genomic DNA and the following primer pairs: for *cpdR*1 (5′-CTCGAGAAGAAGTAGCCACGGCCAGATATGACTGCGAAAAT-3′/5′-CTGCAGATATGTTCGCTGCTCAGGCGGCCAGCATCTTGTT-3′); for *cpdR*2 (5′-CTCGAGAAAAAATACGGGAGGCCATGATGGCGAAAATCCTGATCA-3′/5′-CTGCAGCTATGCATGAATTTTCCCCGGACAGCCCTGCCGCTT-3′); for *clpX*; (5′-GGATCCGGAAGGAAGTGGAAATGAGCAAGGTCAGCGGTA-3′/5′-GCATGCTGTGGCCTCAAGCCGAAACGTTGGTCTTCTCCT-3′). The cloned fragments were sub-cloned in pTH1227, the low-copy-number vector for *S. meliloti* carrying $lacI^q$ and the *tac* promoter (Cheng *et al*., 2007). The resulting plasmids, carrying *cpdR* homologs or *clpX* under the control of *tac* promoter, were mobilized into Rm1021 by tri-parental mating. The cloned *cpdR*1 and *cpdR*2 were converted into *cpdR*1D53A and *cpdR*2D52A by site-directed mutagenesis (Stratagene) with following primer pairs: for *cpdR*1D53A (5′-CCCTTTTCGCTTCTCCTGACCGCCATCGTCATGCCGGAGATGGAC-3′/5′-GTCCATCTCCGGCATGACGATGGCGGTCAGGAGAAGCGAAAAGGG-3′); for *cpdR*2D52A (5′-CCGTTCGACCTCTTGCTATCCGCCATCCGGATGCCGGTCATGGAC-3′/5′-GTCCATGACCGGCATCCGGATGGCGGATAGCAAGAGGTCGAACGG-3′). Underlined nucleotides correspond to mismatches introduced to create the site-directed mutation. The mutated genes were verified by sequencing and cloned in pTH1227 as the same way for the wild-type genes.

Construction of chromosomal *uidA*-transcriptional fusions

To construct *cpdR-uidA* transcriptional fusions, ORFs of *cpdR*1 and *cpdR*2 were amplified by PCR using the following primer pairs: *cpdR1uidA* (5′-ACTAGTTCCCCCATCGGAACCCTTTTTACCATGTCCGGTTCTT-3′/5′-CTCGAGTCAGGCGGCCAGCATCTTGTTGACCTCGTTGACGAGGT-3′); *cpdR*2*uidA* (5′-ACTAGTAGTGGTGACGGGCGACGCAACCTAACTTGGCTCGT-3′/5′-CTCGAGTCAGGCGGCCAGTGCGAGCGCTACGGCCTTGCGGA-3′). The cloned fragments were sub-cloned into the suicide *uidA* reporter vector pJH104. Resulting plasmids were mobilized into Rm1021 by tri-parental mating. Transconjugants were selected on LBMC plates containing Sm and Nm. It must be noted that derivatives of pJH104 were inserted into directly (0 bp) downstream of native gene loci by single crossover recombination without disrupting the genes (ATG of the *uidA* gene is located 23 bp

downstream of the stop codon of each *cpdR* homolog). Although the insertion of pJH104 derivatives results in an additional copy of *cpdR*1 and *cpdR*2, the second copy of *cpdR* genes lack an upstream promoter. Insertions of pJH104 were confirmed by PCR. To construct a *clpX-uidA* transcriptional fusion, the *clpX* ORF and the downstream region of *clpX* were amplified separately by PCR using following primer pairs: *clpXuidA* (5′-TCTAGAGGAAGGAAGTGGAAATGAGCAAGGTCAGCGGTA-3′/5′-GGATCCTGTGGCCTCAAGCCGAAACGTTGGTCTTCTCCT-3′); the downstream region of *clpX* (5′-CCCGGGAGGAGAAGACCAACGTTTCGGCTTGAGGCCACA-3′/5′-CTCGAGTCTCGGCACGCGACCGTCCTTCGACCAGAACCT-3′). Two fragments were sub-cloned together in pJQ200-SK and combined with *uidA*-Nm^r cassette from pWM6 (Metcalf and Wanner, 1993). The resulting pJQ200-SK derivative carries *clpX* followed by *uidA*-Nm^r cassette and the downstream sequence of native *clpX* locus (ATG of the *uidA* gene is located 59 bp downstream of the stop codon of *clpX*). The resulting plasmid was integrated into Rm1021 by double crossover as described above. Thus, in resulting strains, *uidA* is inserted downstream of the stop codons of chromosomal *cpdR*1, *cpdR*2 and *clpX*, being transcribed as the single transcriptional units with *cpdR* homologs and *clpX*.

β-glucuronidase assay in free-living Rm1021 strains

The relative expression level of each *uidA* transcriptional fusion was determined by assaying β-glucuronidase activity as previously described (Jefferson *et al*., 1986) with the following modifications. The assay buffer was supplemented with 10 mM EDTA (pH 8.0) and 0.1% sarcosyl, and the enzyme assays were performed with 5 mM p-nitrophenyl β-D-glucuronide substrate (Sigma). The β-glucuronidase activity was normalized to the cell density ($^{1cm}OD_{600}$) and represented in Miller's unit (Miller, 1972).

Nodulation assay and β-glucuronidase assay in nodules

Seedlings of alfalfa (*Medicago sativa* cv. Iroquois: Agway Inc., Plymouth IN, USA) were inoculated with Rm1021 derivatives on Petri dishes containing Jensen agar as described previously (Leigh *et al*., 1985; Pellock *et al*., 2000). Four-week-old plants were examined for the symbiotic phenotypes. For β-glucuronidase assay, four-weeks-old nodules were excised, hand-sectioned longitudinally in half, and incubated in X-gluc staining buffer [1 mM 5-bromo-4-chloro-3-indoyl-β-d-glucuronide, 0.1 M Na-phosphate buffer (pH 7), 10 mM EDTA, 0.5 mM K-Ferricyanide, 0.5 mM K-Ferrocyanide, 0.1% Triton X-100] at 37°C for overnight. Plants inoculated with Rm1021 derivatives containing pJH104 insertions showed a wild-type phenotype for nodulation.

Construction for tagging CpdR1, CpdR2 and ClpX with YFP

For tagging CpdR1 and CpdR2 with YFP, we fused plasmid-born *cpdR1* and *cpdR2* with *yfpmut*2*A206K*, encoding the *A206K* missense mutation generating monomeric YFP, of pKL183 (Lemon and Grossman, 2000). *cpdR* homologs (including the promoter region and the entire ORF except the stop codon) were amplified by PCR using the following primer pairs: *cpdR1-yfpmut*2 (5′-AAGCTTGATCGAGGCGCGACTGGTCGAGAAAGAACTGGGGA-3′/5′-CTCGAGGGCGGCCAGCATCTTGTTGACCTCGTTGACGAGGT-3′); *cpdR2-yfpmut*2 (5′-AAGCTTAGTGGTGACGGGCGACGCAACCTAACTTGGCTCGT-3′/5′-CTCGAGGGCGGCCAGTGCGAGCGCTACGGCCTTGCGGATGT-3′). The cloned fragments were sub-cloned into the *Hind*III-*Xho*I sites of pTH1227, removing *lacI*q and the *tac* promoter from pTH1227, and combined with the *Xho*I-*Pst*I fragment containing *yfpmut*2*A206K*. The resulting pTH1227 derivatives, carrying the *cpdR1*- or *cpdR2-yfpmut*2*A206K* fusion gene under the control of native promoters of *cpdR*1 or *cpdR*2, were mobilized into the wild-type Rm1021 by tri-parental mating. For tagging ClpX with YFP, we fused chromosomal *clpX* with *yfpmut*2*A206K*. The 3′ region of *clpX* coding sequence

was amplified by PCR using the following primer pair: *clpX-yfpmut2* (5′-GGGCCCTCGACAAGATTTCCCGTAAGTCCGACAACCCGT-3′/5′-GTCGACAGCCGAAACGTTGGTCTTCTCCTCGGAACGCT-3 ′). The cloned fragments was sub-cloned in pJQ200-SK and combined with the *Xho*I-*Pst*I fragment containing *yfpmut2A206K*. The resulting pJQ200-SK derivative, carrying the 3′ region of *clpX* fused to *yfpmut2A206K*, was integrated into the native *clpX* locus by single-cross over, disrupting the wild-type *clpX* locus. The resulting *S. meliloti* strain carries the *clpX-yfpmut2* fusion gene as only one copy of functional *clpX*. We noticed that *S. meliloti* carrying *sacB* gene is symbiotically defective and therefore isolated a spontaneous *sacB*$^{-}$ strain for *in planta* assay.

Live cell microscopy

Aliquots of cells grown in M9 medium supplemented with succinate were stained with the vital membrane dye FM4-64 (Molecular Probes). The following Chroma filter sets were used: 41029 for YFP and 41002C for FM4-64. Exposure time for CpdR1-YFP, CpdR2-YFP and ClpX-YFP fusion protein was 1000, 1000 and 250 milliseconds, respectively. In the case of ClpX-YFP in the *cpdR*1-null background, 6000 milliseconds of exposure was required to capture the distinctive foci. Images were acquired, colorized, and merged using OpenLab software (Improvision). To assess the effect of the growth phases in free-living cells, aliquots of M9 cultures of stationary phase ($^{1cm}OD_{600}$ of >1.5) or log-phase ($^{1cm}OD_{600}$ of 0.4–0.6) were observed under the microscope. For bacteroids, whole alfalfa plants on Petri dishes containing Jensen agar were harvested four weeks after inoculation. Nodules were immediately harvested, crushed and bacteroids were observed by microscopy. Positions of foci were scored after colorization and merging of microscopic images. All data presented here are cumulative from at least two independent experiments, each of which gave nearly identical results.

Flow cytometry

For flow cytometry analyses, *S. meliloti* strains were grown to the mid-logarithmic phase in LBMC. The cells were fixed in 90% ethanol for 16 hours at 4°C, incubated in the sodium citrate buffer (50mM sodium citrate with 3.3 μg ml^{-1} RNase H) for 3 hours at 50°C and stained by Cytox Green (1:6000 diluted in the sodium citrate buffer) (Molecular Probes). For each flow cytometry experiment, the DNA content was measured in a population of 50,000 cells with a Becton Dickinson FACScan machine at 530 nm. The data were collected and analyzed by using the FlowJo software (Tree Star).

Supplementary Material

Refer to Web version on PubMed Central for supplementary material.

Acknowledgments

We are indebted to Mary Lou Pardue (Massachusetts Institute of Technology) and Alan D. Grossman (Massachusetts Institute of Technology) for the use of their microscopes. We are grateful to Jiujun Cheng and Turlough M. Finan (McMaster University) for providing us pTH1218 and pTH1227. We wish to thank Judith Carlin and Marianne White for their help. The authors thank Mary Ellen Wiltrout for insightful discussions and kind suggestions; Celeste Peterson, Glenn Paradis and Michiko E. Taga for help with flow cytometry; Melanie Barker-Berkmen for help with the microscopy.

This work was supported by National Institutes of Health grant GM31010 (to G.C.W.), National Cancer Institute (NCI) Grant CA21615-27 (to G.C.W), MIT Center for Environmental Health Sciences NIEHS P30 ES002109, JSPS Postdoctoral Fellowships for Research Abroad (to H.K.) and a postdoctoral fellowship from the NCI (to L.A.S.) and a Jane Coffin Childs Memorial Fund Fellowship (to P.C.) and NIH Grant 5K99GM084157-01 (to P.C.). G.C.W. is an American Cancer Society Research Professor.

References

Baker TA, Sauer RT. ATP-dependent proteases of bacteria: recognition logic and operating principles. Trends Biochem Sci. 2006; 31:647–653. [PubMed: 17074491]

Barnett MJ, Hung DY, Reisenauer A, Shapiro L, Long SR. A homolog of the CtrA cell cycle regulator is present and essential in *Sinorhizobium meliloti*. J Bacteriol. 2001; 183:3204–3210. [PubMed: 11325950]

Bellefontaine AF, Pierreux CE, Mertens P, Vandenhaute J, Letesson JJ, De Bolle X. Plasticity of a transcriptional regulation network among alpha-proteobacteria is supported by the identification of CtrA targets in *Brucella abortus*. Mol Microbiol. 2002; 43:945–960. [PubMed: 11929544]

Biondi EG, Reisinger SJ, Skerker JM, Arif M, Perchuk BS, Ryan KR, Laub MT. Regulation of the bacterial cell cycle by an integrated genetic circuit. Nature. 2006; 444:899–904. [PubMed: 17136100]

Brewin, NJ. Tissue and cell invasion by *Rhizobium*: The structure and development of infection threads and symbiosis. In: Spaink, HP.; Kondorosi, A.; Hooykaas, PJJ., editors. The Rhizobiaceae. Dordrecht, Boston, London: Kluwer Acad Press; 1998. p. 417-429.

Broughton WJ, Jabbouri S, Perret X. Keys to symbiotic harmony. J Bacteriol. 2000; 182:5641–5652. [PubMed: 11004160]

Campbell GRO, Reuhs BL, Walker GC. Chronic intracellular infection of alfalfa nodules by *Sinorhizobium meliloti* requires correct lipopolysaccharide core. Proc Natl Acad Sci U S A. 2002; 99:3938–3943. [PubMed: 11904442]

Cheng J, Sibley CD, Zaheer R, Finan TM. A *Sinorhizobium meliloti minE* mutant has an altered morphology and exhibits defects in legume symbiosis. Microbiology. 2007; 153:375–387. [PubMed: 17259609]

Chien P, Perchuk BS, Laub MT, Sauer RT, Baker TA. Direct and adaptor-mediated substrate recognition by an essential AAA+ protease. Proc Natl Acad Sci U S A. 2007; 104:6590–6595. [PubMed: 17420450]

Dougan DA, Mogk A, Zeth K, Turgay K, Bukau B. AAA+ proteins and substrate recognition, it all depends on their partner in crime. FEBS Lett. 2002; 529:6–10. [PubMed: 12354604]

Duerig A, Abel S, Folcher M, Nicollier M, Schwede T, Amiot N, Giese B, Jenal U. Second messenger-mediated spatiotemporal control of protein degradation regulates bacterial cell cycle progression. Genes Dev. 2009; 23:93–104. [PubMed: 19136627]

Ebeling S, Kundig C, Hennecke H. Discovery of a rhizobial RNA that is essential for symbiotic root nodule development. J Bacteriol. 1991; 173:6373–6382. [PubMed: 1717438]

Ferguson GP, Datta A, Carlson RW, Walker GC. Importance of unusually modified lipid A in *Sinorhizobium* stress resistance and legume symbiosis. Mol Microbiol. 2005; 56:68–80. [PubMed: 15773979]

Flynn JM, Neher SB, Kim YI, Sauer RT, Baker TA. Proteomic discovery of cellular substrates of the ClpXP protease reveals five classes of ClpX-recognition signals. Mol Cell. 2003; 11:671–683. [PubMed: 12667450]

Fellay R, Frey J, Krisch H. Interposon mutagenesis of soil and water bacteria: a family of DNA fragments designed for *in vitro* insertional mutagenesis of Gram-negative bacteria. Gene. 1987; 52:147–154. [PubMed: 3038679]

Foucher F, Kondorosi E. Cell cycle regulation in the course of nodule organogenesis in *Medicago*. Plant Mol Biol. 2000; 43:773–786. [PubMed: 11089876]

Gage DJ. Analysis of infection thread development using Gfp- and DsRed-expressing *Sinorhizobium meliloti*. J Bacteriol. 2002; 184:7042–7046. [PubMed: 12446653]

Gage DJ. Infection and invasion of roots by symbiotic, nitrogen-fixing rhizobia during nodulation of temperate legumes. Microbiol Mol Biol Rev. 2004; 68:280–300. [PubMed: 15187185]

Gage DJ, Margolin W. Hanging by a thread: invasion of legume plants by rhizobia. Curr Opin Microbiol. 2000; 3:613–617. [PubMed: 11121782]

Gibson KE, Kobayashi H, Walker GC. Molecular determinants of a symbiotic chronic infection. Annu Rev Genet. 2008; 42:413–441. [PubMed: 18983260]

Gorbatyuk B, Marczynski GT. Regulated degradation of chromosome replication proteins DnaA and CtrA in *Caulobacter crescentus*. Mol Microbiol. 2005; 55:1233–1245. [PubMed: 15686567]

Gottesman S, Roche E, Zhou Y, Sauer RT. The ClpXP and ClpAP proteases degrade proteins with carboxy-terminal peptide tails added by the SsrA-tagging system. Genes Dev. 1998; 12:1338–1347. [PubMed: 9573050]

Hallez R, Bellefontaine AF, Letesson JJ, De Bolle X. Morphological and functional asymmetry in alpha-proteobacteria. Trends Microbiol. 2004; 12:361–365. [PubMed: 15276611]

Herman C, Thevenet D, Bouloc P, Walker GC, D'Ari R. Degradation of carboxy-terminal-tagged cytoplasmic proteins by the *Escherichia coli* protease HflB (FtsH). Genes Dev. 1998; 12:1348–1355. [PubMed: 9573051]

Iniesta AA, McGrath PT, Reisenauer A, McAdams HH, Shapiro L. A phospho-signaling pathway controls the localization and activity of a protease complex critical for bacterial cell cycle progression. Proc Natl Acad Sci U S A. 2006; 103:10935–10940. [PubMed: 16829582]

Iniesta AA, Shapiro L. A bacterial control circuit integrates polar localization and proteolysis of key regulatory proteins with a phospho-signaling cascade. Proc Natl Acad Sci U S A. 2008; 105:16602–16607. [PubMed: 18946044]

Jenal U, Fuchs T. An essential protease involved in bacterial cell-cycle control. Embo J. 1998; 17:5658–5669. [PubMed: 9755166]

Jenal U, Hengge-Aronis R. Regulation by proteolysis in bacterial cells. Curr Opin Microbiol. 2003; 6:163–172. [PubMed: 12732307]

Jones KM, Kobayashi H, Davies BW, Taga ME, Walker GC. How rhizobial symbionts invade plants: the *Sinorhizobium-Medicago* model. Nat Rev Microbiol. 2007; 5:619–633. [PubMed: 17632573]

Kaminski, PA.; Batut, J.; Boistard, P. A survey of symbiotic nitrogen fixation by rhizobia. In: Spaink, HP.; Kondorosi, A.; Hooykaas, PJJ., editors. The Rhizobiaceae. Dordrecht, Boston, London: Kluwer Acad Press; 1998. p. 431-460.

Kain J, He GG, Losick R. Polar localization and compartmentalization of ClpP proteases during growth and sporulation in *Bacillus subtilis*. J Bacteriol. 2008; 190:6749–57. [PubMed: 18689476]

Keiler KC, Waller PR, Sauer RT. Role of a peptide tagging system in degradation of proteins synthesized from damaged messenger RNA. Science. 1996; 271:990–993. [PubMed: 8584937]

Kirstein J, Strahl H, Moliere N, Hamoen LW, Turgay K. Localization of general and regulatory proteolysis in *Bacillus subtilis* cells. Mol Microbiol. 2008; 70:682–94. [PubMed: 18786145]

Kobayashi, H.; Broughton, WJ. Fine-tuning of symbiotic genes in rhizobia: Flavonoid signal transduction cascade. In: Dilworth, MJ.; James, EK.; Sprent, JI.; Newton, WE., editors. Nitrogen Fixation: Origins, Applications, and Research Progress Volume 7: Nitrogen-fixing Legume Symbiosis. Springer; Netherlands: 2008. p. 117-152.

Kobayashi H, Sunako M, Hayashi M, Murooka Y. DNA synthesis and fragmentation in bacteroids during *Astragalus sinicus* root nodule development. Biosci Biotechnol Biochem. 2001; 65:510–515. [PubMed: 11330661]

Lam H, Matroule JY, Jacobs-Wagner C. The asymmetric spatial distribution of bacterial signal transduction proteins coordinates cell cycle events. Dev Cell. 2003; 5:149–159. [PubMed: 12852859]

Laub MT, Chen SL, Shapiro L, McAdams HH. Genes directly controlled by CtrA, a master regulator of the *Caulobacter* cell cycle. Proc Natl Acad Sci U S A. 2002; 99:4632–4637. [PubMed: 11930012]

Laub MT, McAdams HH, Feldblyum T, Fraser CM, Shapiro L. Global analysis of the genetic network controlling a bacterial cell cycle. Science. 2000; 290:2144–2148. [PubMed: 11118148]

Leigh JA, Signer ER, Walker GC. Exopolysaccharide-deficient mutants of *Rhizobium meliloti* that form ineffective nodules. Proc Natl Acad Sci U S A. 1985; 82:6231–6235. [PubMed: 3862129]

Lemon KP, Grossman AD. Movement of replicating DNA through a stationary replisome. Mol Cell. 2000; 6:1321–1330. [PubMed: 11163206]

Liu J, Cosby WM, Zuber P. Role of Lon and ClpX in the post-translational regulation of a sigma subunit of RNA polymerase required for cellular differentiation in *Bacillus subtilis*. Mol Microbiol. 1999; 33:415–428. [PubMed: 10411757]

Margolin W. FtsZ and the division of prokaryotic cells and organelles. Nat Rev Mol Cell Biol. 2005; 6:862–871. [PubMed: 16227976]

McGrath PT, Iniesta AA, Ryan KR, Shapiro L, McAdams HH. A dynamically localized protease complex and a polar specificity factor control a cell cycle master regulator. Cell. 2006; 124:535–547. [PubMed: 16469700]

Meade HM, Long SR, Ruvkun GB, Brown SE, Ausubel FM. Physical and genetic characterization of symbiotic and auxotrophic mutants of *Rhizobium meliloti* induced by transposon Tn5 mutagenesis. J Bacteriol. 1982; 149:114–122. [PubMed: 6274841]

Mergaert P, Uchiumi T, Alunni B, Evanno G, Cheron A, Catrice O, Mausset AE, Barloy-Hubler F, Galibert F, Kondorosi A, Kondorosi E. Eukaryotic control on bacterial cell cycle and differentiation in the *Rhizobium*-legume symbiosis. Proc Natl Acad Sci U S A. 2006; 103:5230–5235. [PubMed: 16547129]

Metcalf WW, Wanner BL. Construction of new beta-glucuronidase cassettes for making transcriptional fusions and their use with new methods for allele replacement. Gene. 1993; 129:17–25. [PubMed: 8335256]

Miller, JF. Experiments in Molecular Genetics. New York: Cold Spring Harbor Laboratory, Cold Spring Harbor; 1972.

Oke V, Long SR. Bacteroid formation in the *Rhizobium*-legume symbiosis. Curr Opin Microbiol. 1999; 2:641–646. [PubMed: 10607628]

Pellock BJ, Cheng HP, Walker GC. Alfalfa root nodule invasion efficiency is dependent on *Sinorhizobium meliloti* polysaccharides. J Bacteriol. 2000; 182:4310–4318. [PubMed: 10894742]

Perret X, Staehelin C, Broughton WJ. Molecular basis of symbiotic promiscuity. Microbiol Mol Biol Rev. 2000; 64:180–201. [PubMed: 10704479]

Prell J, Poole P. Metabolic changes of rhizobia in legume nodules. Trends Microbiol. 2006; 14:161–168. [PubMed: 16520035]

Quandt J, Hynes MF. Versatile suicide vectors which allow direct selection for gene replacement in gram-negative bacteria. Gene. 1993; 127:15–21. [PubMed: 8486283]

Quon KC, Marczynski GT, Shapiro L. Cell cycle control by an essential bacterial two-component signal transduction protein. Cell. 1996; 84:83–93. [PubMed: 8548829]

Quon KC, Yang B, Domian IJ, Shapiro L, Marczynski GT. Negative control of bacterial DNA replication by a cell cycle regulatory protein that binds at the chromosome origin. Proc Natl Acad Sci U S A. 1998; 95:120–125. [PubMed: 9419339]

Rodriguez H, Mendoza A, Cruz MA, Holguin G, Glick BR, Bashan Y. Pleiotropic physiological effects in the plant growth-promoting bacterium *Azospirillum brasilense* following chromosomal labeling in the *clpX* gene. FEMS Microbiol Ecol. 2006; 57:217–225. [PubMed: 16867140]

Sauer RT, Bolon DN, Burton BM, Burton RE, Flynn JM, Grant RA, Hersch GL, Joshi SA, Kenniston JA, Levchenko I, Neher SB, Oakes ES, Siddiqui SM, Wah DA, Baker TA. Sculpting the proteome with AAA(+) proteases and disassembly machines. Cell. 2004; 119:9–18. [PubMed: 15454077]

Siam R, Marczynski GT. Cell cycle regulator phosphorylation stimulates two distinct modes of binding at a chromosome replication origin. Embo J. 2000; 19:1138–1147. [PubMed: 10698954]

Simmons LA, Grossman AD, Walker GC. Clp and Lon proteases occupy distinct subcellular positions in *Bacillus subtilis*. J Bacteriol. 2008; 190:6758–6768. [PubMed: 18689473]

Skerker JM, Prasol MS, Perchuk BS, Biondi EG, Laub MT. Two-component signal transduction pathways regulating growth and cell cycle progression in a bacterium: a system-level analysis. PLoS Biol. 2005; 3:e334. [PubMed: 16176121]

Weichart D, Querfurth N, Dreger M, Hengge-Aronis R. Global role for ClpP-containing proteases in stationary-phase adaptation of *Escherichia coli*. J Bacteriol. 2003; 185:115–125. [PubMed: 12486047]

Wright R, Stephens C, Shapiro L. The CcrM DNA methyltransferase is widespread in the alpha subdivision of proteobacteria, and its essential functions are conserved in *Rhizobium meliloti* and *Caulobacter crescentus*. J Bacteriol. 1997; 179:5869–5877. [PubMed: 9294447]

Wright R, Stephens C, Zweiger G, Shapiro L, Alley MR. *Caulobacter* Lon protease has a critical role in cell-cycle control of DNA methylation. Genes Dev. 1996; 10:1532–1542. [PubMed: 8666236]

Zweiger G, Marczynski G, Shapiro L. A *Caulobacter* DNA methyltransferase that functions only in the predivisional cell. J Mol Biol. 1994; 235:472–485. [PubMed: 8289276]

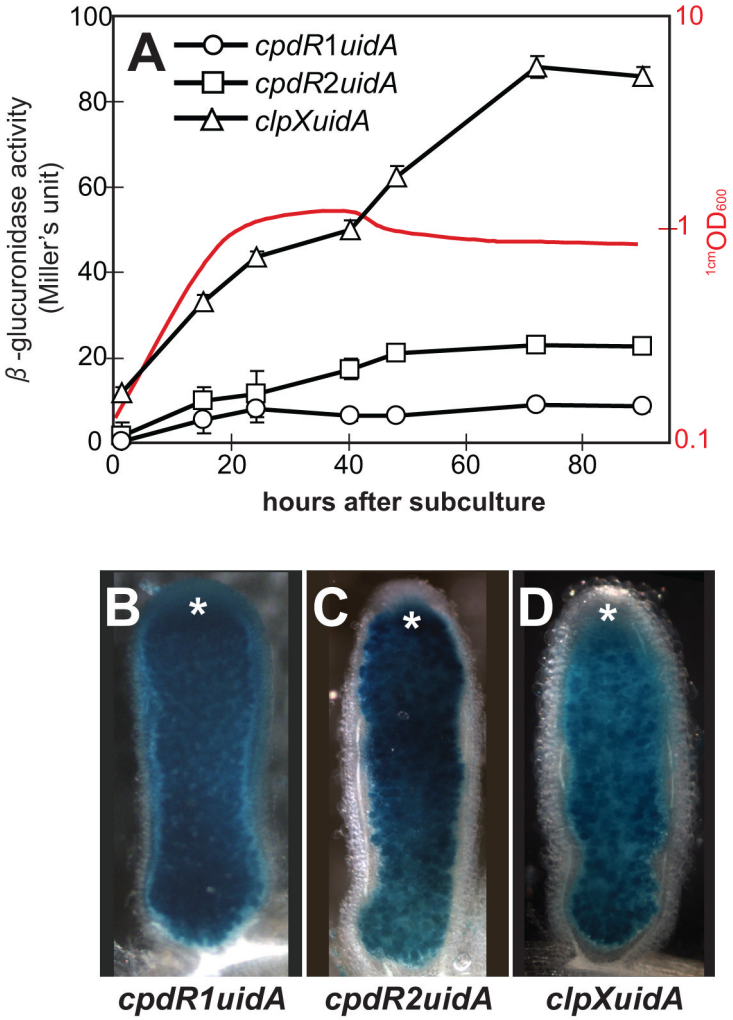

Fig. 1. Expression of *S. meliloti cpdR* and *clpX* homologs in free-living cells and bacteroids

Panels A represents the levels of β-glucuronidase activity (given in Miller's units) for the transcriptional level of *cpdR*1, *cpdR*2 and *clpX* transcriptionally fused to *uidA*, respectively. The wild-type *S. meliloti* Rm1021 showed no β-glucuronidase activity (data not shown). Assays were performed at 1, 16, 24, 40, 48, 72 and 90 hours after subculture. The values reported represent the means of three independent experiments with standard errors (error bars). A growth curve of a representative strain (monitored by $^{1cm}OD_{600}$) is also shown (red curves). Panels B to D represent histochemical localization of β-glucuronidase activity in nodule hand-sections. Nodules were harvested from alfalfa plants infected with *S. meliloti* strains used in Panel A. β-glucuronidase activity was visualized as blue precipitates of the chromogenic substrate 5-bromo-4-chloro-3-indolyl glucuronide (X-Gluc). A total of 30–40 nodules from five plants were examined for each fusion. The meristematic zone of nodule is marked with white asterisks.

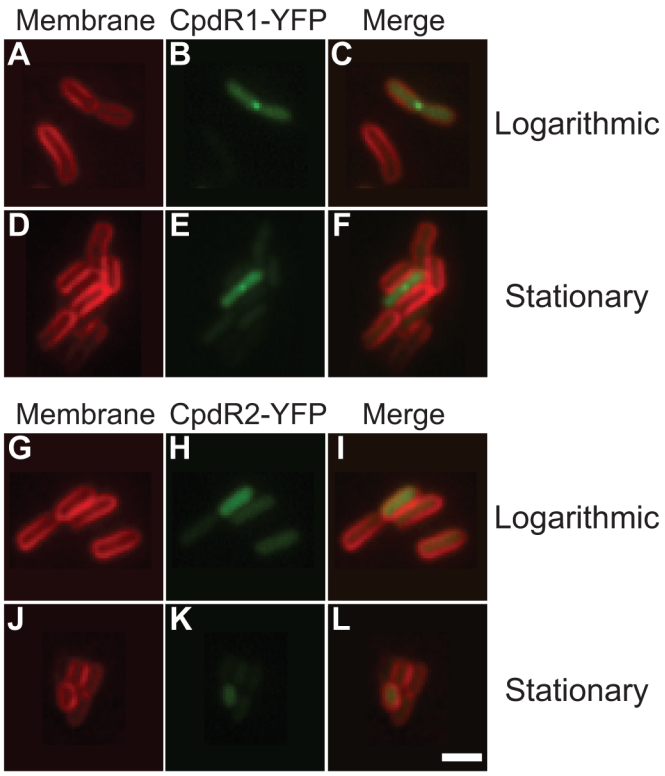

Fig. 2. Subcellular localization of CpdR1 and CpdR2 in free-living *S. meliloti* cells

Panels A to L represent subcellular localization of CpdR1-YFP (A to F) and CpdR2-YFP (G to L) fusion proteins in free-living *S. meliloti* by epi-fluorescence microscopy. *S. meliloti* strains carrying fusion genes were grown in M9 medium supplemented with succinate. Cells were examined in the logarithmic phase (A to C and G to I) or the stationary phase (D to F and J to L). Localization of YFP-fusion proteins was visualized in living cells as represented in green (B, E, H and K). The cell membrane was stained by FM4-64 as represented in red (A, D, G and J). Epi-fluorescence views of different filters were merged to analyze relative localization (C, F, I and L). No focus was observed in cells of the wild-type *S. meliloti* strain Rm1021 (data not shown). Scale bar represents 2 μm.

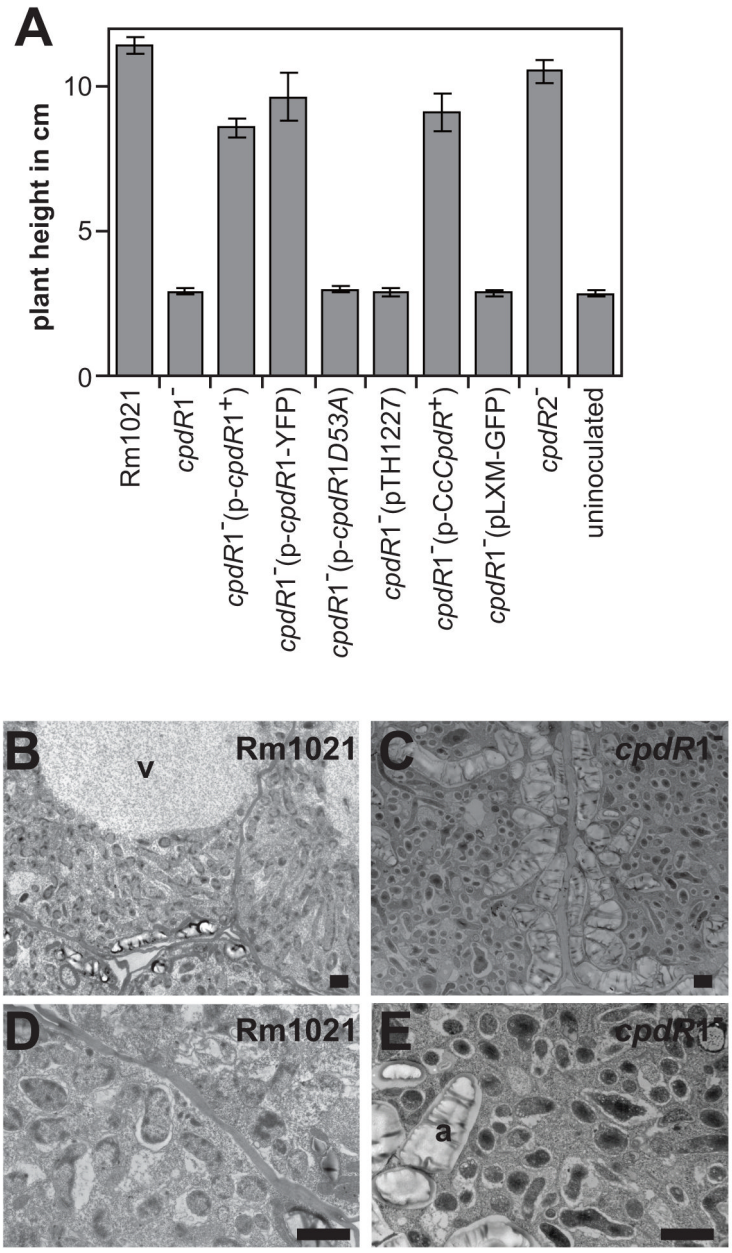

Fig. 3. CpdR1 is critical for symbiosis between *S. meliloti* and alfalfa

(A) The *cpdR*1-null mutant elicits ineffective nodules on alfalfa roots. The symbiotic defect can be complemented by plasmid-born *cpdR*1^{+}, the *cpdR*1-*yfpmut*2 fusion gene and *C. crescentus cpdR* but not by *cpdR*1*D53A* or vector controls (pTH1227 and pLXM-GFP). The disruption of *cpdR*2 has neither a positive nor a negative effect on growth of plants relative to that of the wild-type *S. meliloti* strain Rm1021. Growth of alfalfa plants were examined four weeks after inoculation. The plant heights are the lengths of shoots (cm). Error bars indicate standard errors. At least 20 plants were examined for each strain. (B to E) In nodules elicited by the wild-type *S. meliloti* strain Rm1021 viewed by transmission electron microscopy (B and D), cells from the nitrogen fixing zone are packed with bacteroids and contained a large central vacuole (v). Nodules elicited by the *cpdR*1-null mutant (C and E)

contain plant cells filled with bacteria of irregular-coccoid morphology and have large amyloplasts (a). Scale bars represent 2 μm.

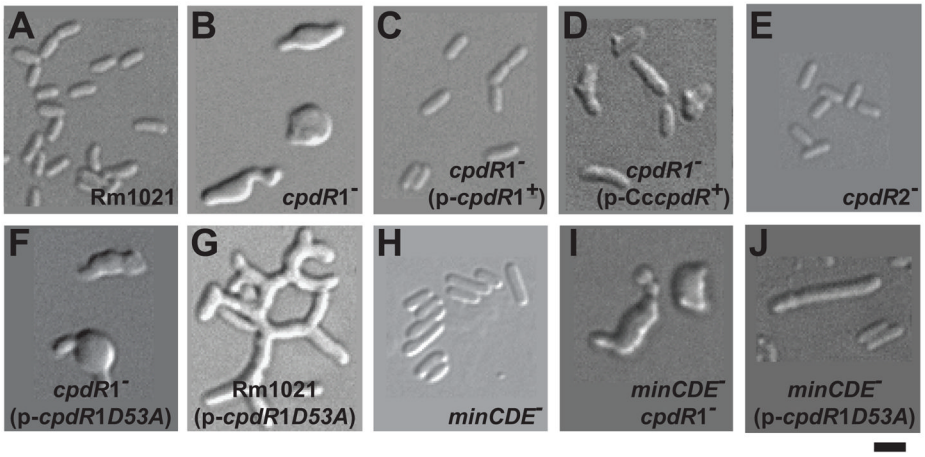

Fig. 4. Cell morphology of *S. meliloti* strains

DIC view of the wild-type *S. meliloti* stain Rm1021 (A), the *cpdR*1-null mutant (B), the *cpdR*1-null mutant carrying p-*cpdR*1$^+$ (C) or p-Cc*cpdR*$^+$ (D), the *cpdR*2-null mutant (E), the *cpdR*1-null mutant (F) or the wild-type strain (G) carrying p-*cpdR*1*D53A*, the *minCDE*-null mutant (H), the *minCDEcpdR*1 double mutant (I) and the *minCDE*-null mutant carrying p-*cpdR*1*D53A*. Cells were grown in LBMC medium to logarithmic phase and processed for DIC microscopy. Scale bars represent 2 μm.

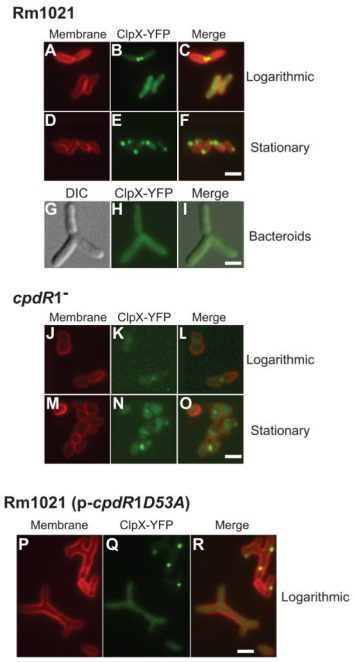

Fig. 5. Subcellular localization of ClpX in cells of *S. meliloti* strains

Panels A to R represent subcellular localization of the ClpX-YFP fusion protein in free-living *S. meliloti* strains (A to F and J to R) or bacteroids (G to I). Localization of ClpX-YFP in free-living cells of the wild-type *S. meliloti* strain Rm1021 (A to F), the *cpdR*1-null mutant (J to O) and the wild-type *S. meliloti* strain Rm1021 carrying p-*cpdR*1*D53A* (P to R) was examined by epi-fluorescence microscopy essentially in the same way as in Figure 2. Panel G to H represent subcellular localization of ClpX-YFP fusion protein in bacteroids of the wild-type *S. meliloti* Rm1021 by epi-fluorescence/DIC microscopy. Nodules were harvested from alfalfa plants infected with Rm1021*clpX-yfp* and immediately crushed. Long, blanched bacteroid cells were visually distinguished from non-differentiated *S. meliloti* cells or plant-derived materials (G). In contrast to the free-living cells, the membrane of bacteroids could not be stained by FM4-64 (data not shown). Localization of ClpX-YFP was visualized in bacteroids as represented in green (H). Epi-fluorescence view and DIC view were merged to analyze relative localization (I). Scale bars represent 2 μm.

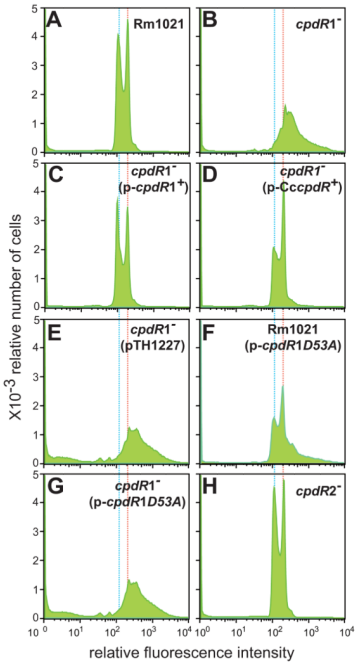

Fig 6. Flow cytometry analyses of *S. meliloti* strains

The DNA contents of *S. meliloti* strains were measured in a population of 50,000 cells with a Becton Dickinson FACScan machine at 530 nm. Relative cell number (y axis) is plotted against the Cytox Green fluorescence signal (arbitrary units). 1C and 2C of the genome equivalents were marked with blue-and red-dotted lines, respectively.

Table 1

Formation of CpdR-YFP foci in *S. meliloti* Rm1021

			% of cells with *n* foci		
	Growth phase	**No. of cells**	**0**	**1**	**2≤**
CpdR1-YFP	Logarithmic	1399	94	6	ND
	Stationary	1273	95	5	ND
CpdR2-YFP	Logarithmic	534	100	ND	ND
	Stationary	561	99	<1	ND

Table 2

Formation of highly branched cells in *S. meliloti* Rm1021 strains

		% of cells with morphology		
Strains	**No. of cells**	**rod**	**elongated**	**highly branched**
Rm1021(pTH1227)	413	99	1<	ND
Rm1021*minCDE*⁻(pTH1227)	453	99	1<	ND
Rm1021(p-*cpdR*1D53A)	551	82	12	6
Rm1021*minCDE*⁻(p-*cpdR1D53A*)	405	90	10	ND

“rod”, 1–3 μm rod-shape with two poles; “elongated”, cells longer than 4 μm with two to three poles; “highly branched”, cells with more than three poles.

Table 3

Growth phase-dependent formation of ClpX-YFP foci in *S. meliloti* strains

			Percentage of cells with *n* foci		
***S. meliloti* strain**	**Growth phase**	**No. of cells**	**0**	**1**	**2≤**
Rm1021	Logarithmic	1005	90	9	1
	Stationary	594	12	84	4
	Bacteroid	579	99	1	ND
Rm1021*cpdR*1ΩSp^r	Logarithmic	545	94	5	<1
	Stationary	1004	88	11	<1
Rm1021*cpdR*2::*uidA*-Cm^r	Logarithmic	938	91	8	<1
	Stationary	869	21	76	3
Rm1021(p-*cpdR*1*D53A*)	Logarithmic	798	91	8	1
Rm1021(p-*cpdR*2*D52A*)	Logarithmic	677	88	11	1